arXiv:astro-ph/0308548v2 29 Aug 2003

Asymmetric Planetary Nebulae III
ASP Conference Series, Vol. XXX, 2004
M. Meixner, J. Kastner, and N. Soker eds.

The Last Hurrah: PPN Formation by a Magnetic Explosion

Sean Matt[1]

Physics & Astronomy Department, McMaster University, Hamilton ON, Canada L8S 4M1

Adam Frank and Eric Blackman

Physics & Astronomy Department, University of Rochester, Rochester NY, U.S.A. 14627

Abstract. We discuss a mechanism by which a giant star can expel its envelope in an outburst, leaving its core exposed. The outburst is powered by rotational kinetic energy of the core, transferred to the envelope via the twisting of magnetic fields. We show that, if the core is magnetized, and if it has sufficient angular momentum, this mechanism may be triggered at the end of the asymptotic giant branch phase, and drive a proto-planetary nebula (pPN) outflow. This explosion of magnetic energy self-consistently explains some of the asymmetries and dynamics of pPNe.

1. Introduction

The formation and shaping of planetary nebulae (PNe) has been described by a generalized interacting stellar wind (GISW) model (Kwok et al., 1978; Balick, 1987), in which the central star of a PN produces a fast wind that interacts with the slower moving, previously ejected, asymptotic giant branch (AGB) wind. According to the GISW model, both the slow and fast winds are driven by radiation, and asymmetric PN shapes result from asymmetries in the slow, AGB wind, from magnetic effects in the shocked fast wind (e.g., Chevalier & Luo, 1994; García-Segura et al., 1999, see also García-Segura in these proceedings), or from some combination of the two.

However, some recent observations of proto-planetary nebulae (pPNe, precursors of PNe) call for a revolutionary change in our understanding of the driving and shaping of post-AGB outflows. These observations are as follows:

1. The material ejected during the pPN phase is highly structured, often containing multiple apparent ejection axes and occasionally appearing quite chaotic (e.g., Balick & Frank, 2002). Several pPNe (e.g., CRL 2688, OH231.8+4.2, IRAS 17150-3224, and IRAS 17441-2411) exhibit quadrupolar symmetry, consisting of outflowing disks—dense enough to obscure central starlight—and bipolar lobes or jets.

[1]CITA National Fellow

2. Spherical shells of reflected starlight often surrounding highly structured PNe and pPNe (e.g., Terzian & Hajian, 2000; Balick et al., 2001, see also Su in these proceedings). This suggests that the AGB wind is spherically symmetric, and so it cannot be responsible for the asymmetry in subsequent flows. Thus, pPN outflows must be self-shaped.
3. The momentum carried in pPN outflows is often a few orders of magnitude larger than can be explained by radiation pressure driving (Knapp, 1986; Bujarrabal et al., 2001, see also Bujarrabal in these proceedings), so a new and more powerful wind driving mechanism is needed.
4. The pPN phase is extremely short lived, typically only a few hundred years. Yet the observed flows often follow a "Hubble law" expansion ($v \propto R$, e.g., Alcolea et al., 2001), suggesting that ejecta accelerate in a short time compared to the pPN lifetime, and afterward follow ballistic trajectories. Therefore, the flows are really outbursts, transient winds where the momentum and kinetic energy suddenly and temporarily increase.

Together, these key observations seem to require a new ejection mechanism that is quasi-explosive, is triggered at the end of the AGB phase, and produces intrinsically asymmetric flow structures.

Here we show that the rotational kinetic energy of the core of an AGB star can be converted to linear kinetic energy and transferred to the envelope. The conversion and transferral of energy happens via the twisting of magnetic fields anchored in the core, and naturally results in a complete and asymmetric ejection of the envelope. The acceleration of the envelope occurs in a very short time compared to the typical age of pPNe. We will describe the conditions necessary for such an ejection to take place and discuss how stars may achieve those conditions near the end of the AGB phase. Our model is general and may be relevant to other classes of objects, such as SNe, GRB's, and η Carinae.

2. The Magnetic Explosion

Consider an AGB star with a slowly contracting core and an expanding, convective envelope. If the star is rotating at all, angular momentum conservation requires that there will be a region of differential rotation at the interface between the core and the envelope. Blackman et al. (2001) have shown that the differential rotation in an AGB star can drive a solar-like magnetic dynamo, in which magnetic fields are amplified to an (time-averaged) equilibrium value of 10^4–10^6 Gauss at the interface. The magnetic field is mixed by convection throughout the envelope. Whether a binary interaction is required to maintain (or trigger) differential rotation in AGB stars remains an open question.

Large mass loss rates from the envelope, during the late stages of the AGB phase, result in a slow expansion of the envelope and a decrease in its density at all depths. As the weight of the overlying envelope decreases, the relative importance of the magnetic field increases. In particular, there may be a threshold at which the magnetic (plus thermal) energy within the envelope exceeds its gravitational potential energy. At that point, the envelope as a whole would be driven off in a single, short-lived event.

Due to the extreme difficulty of modeling, self-consistently, the complex interface dynamo, together with a proper treatment of the turbulent envelope

and mass loss from the top of the convection zone, we consider here a slightly different and simplified situation. Rather than having an envelope with a constant magnetic energy and a decreasing density, we consider a constant density envelope in which the magnetic energy increases. Due to our simplifications, the magnetic energy is generated in a short time and only at the interface between the core and envelope, where strong differential rotation twists up pre-existing poloidal magnetic fields. Though the magnetic energy is produced only at the base of the envelope (and not mixed everywhere throughout), we expect the same qualitative behavior described above, where the magnetic energy exceeds the gravitational potential energy, and the envelope is driven off in an outburst.

For this initial study, we have carried out time-dependent, numerical magnetohydrodynamic (MHD) simulations. We use the simulation code of Matt (2002), which employs a finite difference scheme to solve the standard, adiabatic ($\gamma = 5/3$), ideal MHD equations, plus source terms for gravity, on an Eulerian, cylindrical (r, z), nested grid. The code assumes axisymmetry (where $\delta/\delta\phi$ of all quantities $= 0$). We use "outflow" boundary conditions (BCs) on the outermost boundary (though material doesn't leave the grid by the end of the simulations), and assume reflection symmetry about the equator ($z = 0$). The simulation domain, then, consists of an r–z slice through a single quadrant, with the stellar core specified by a circular, inner BC.

For simplicity, we want to ignore effects of a wind from the core, so we have chosen a "solid" BC such that no matter can flow from or onto the core. The core behaves as a perfect electric conductor and initially is rotating as a solid body and is threaded by a rotation-axis aligned dipole magnetic field. The computational domain (existing between the core boundary and the outer boundary) is initialized with a hydrostatic envelope whose density falls off as R^{-2} (where R is the spherical radius). The envelope is initially stagnant (no rotation or motion) and is threaded everywhere by the dipole magnetic field that is anchored to the core. We also assume that the mass of the core is much greater than that of the envelope, so that the envelope's self-gravity can be ignored.

The upper left panel of figure 1 shows the initial configuration in the inner part of the computational domain (from the center, out to 13 core radii, $R_{\rm core}$). The initial configuration is static and in equilibrium. At $t = 0$ the core begins to rotate. Differential rotation between the core and stagnant envelope leads to an azimuthal twisting of the dipole field lines just above the core. The azimuthal magnetic field B_ϕ increases linearly in time, until it becomes strong enough to be dynamically important. At that time, magnetic pressure forces (i.e., $-\nabla B_\phi^2$), begin to drive material outward, away from the core.

In our chosen configuration, the key parameters are the relative values of the characteristic speeds in the system—the equatorial rotation speed of the core ($v_{\rm rot}$), the initial Alfvén speed at the core equator ($v_{\rm A}$), and the escape speed from the surface of the core ($v_{\rm esc}$)—which are related to the relative values of various energies in the system. Note that in hydrostatic equilibrium, the sound speed is proportional to the escape speed, so the sound speed (or thermal energy) is not a key, independent parameter. Here, we present a case with $v_{\rm rot}/v_{\rm esc} = 0.1$ (14% of breakup rotation) and $v_{\rm A}/v_{\rm esc} = 1.0$.

The upper right, lower left, and lower right panels of figure 1 show the evolution after 1.5, 3.0, and 4.5 rotations of the core, respectively. The expansion

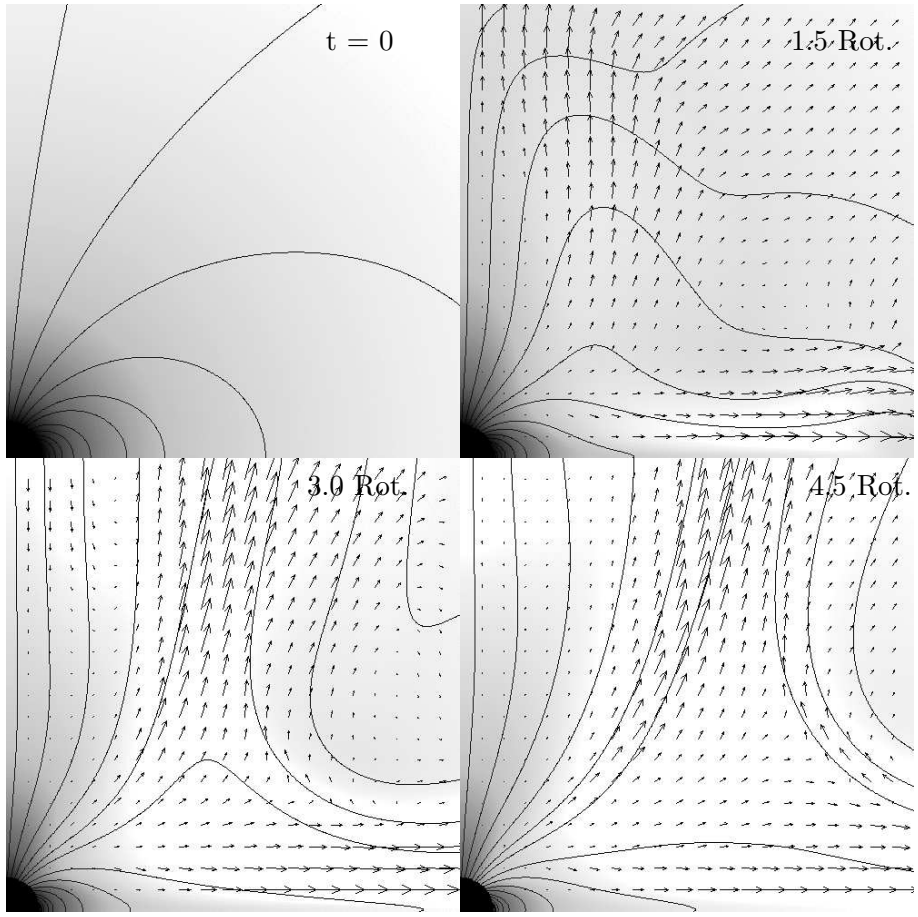

Figure 1. Greyscale images of log density (black is highest density), poloidal field lines, and velocity vectors show the evolution of the system in the region near the core, spanning $0 \leq r$, $z \leq 13R_{\rm core}$. The core is in the lower left of each panel, and the rotation axis is vertical.

of newly generated azimuthal magnetic field is evident in the figure, as it drives the envelope material outward. This also leads to an expansion of the poloidal magnetic field (lines), though some field lines near the equator remain closed, where material is forced and held in corotation with the core. Due to the coupling of the rotation to the dipole field, B_ϕ has a maximum near the core at mid latitudes. Thus, magnetic pressure forces point (from strong to weak field), not only radially away from the core, but also toward the rotation axis and toward the magnetic equator. This produces structures in the outburst such that the expansion is faster toward the equatorial and polar directions. Finally, notice that the density near the core decreases with time. This is because that region is drained of material by the expansion of the magnetic field (our "solid" core BC prevents the region from being replenished by mass flow from the core). This process is truly a transient phenomenon.

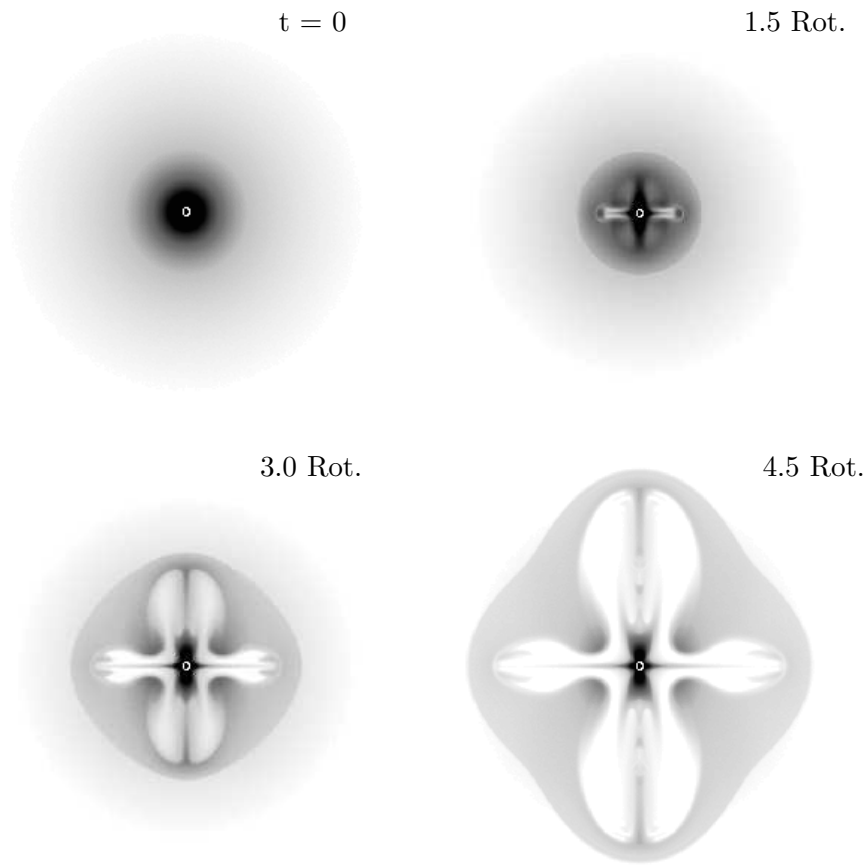

Figure 2. Greyscale images of log density (black is highest density) show the evolution of the system far from the core, spanning $-130R_{\rm core} \leq r,\ z \leq 130R_{\rm core}$. The core is indicated by a white circle in the center of each panel, and the rotation axis is vertical.

The four panels of figure 2 show the evolution of the system at the same times and for the same simulation as in figure 1. However, the data in figure 2 is shown on a scale that is 10 times larger than in figure 1 (by taking advantage of nested simulation grids), and the data has been reflected about the rotation axis and equator to better illustrate the flow.

As the simulation proceeds, one sees a swept up shell of envelope material moving outward from the core. In the upper right panel, the outer edge of this shell is quite spherical, and it represents the initial pressure wave expanding outward to make room for the expanding magnetic field. As the field expansion accelerates and exceeds the sound speed, it overtakes the spherical pressure wave and begins to protrude outward along the rotation axis and magnetic equator. This is evident in the bottom two panels, where the outer dense region is swept up envelope material, and the "hollow" inner region is actually filled with magnetic (mostly B_ϕ) energy. Note the strongly quadrupolar shape of

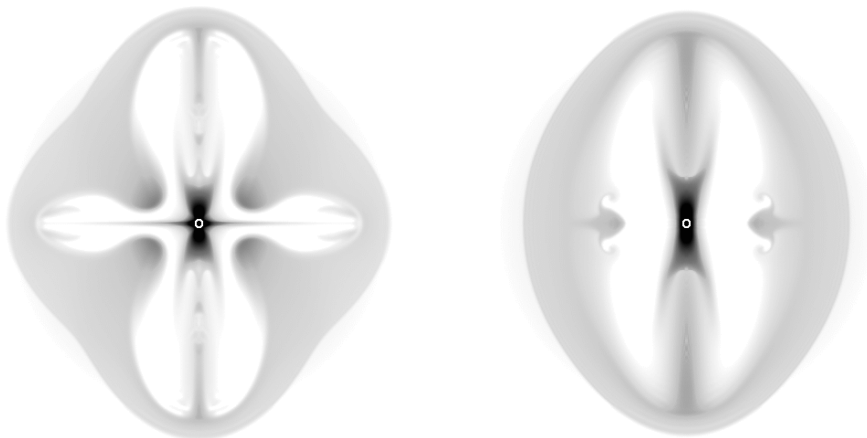

Figure 3. Case with initial dipole magnetic field (left) compared to a case with initial split monopole (right). The panels have the same spatial and density scale as figure 2.

this inflating bubble. Again, the asymmetry is due to the fact that a spinning dipole produces a B_ϕ that is strongest at mid latitudes, so magnetic pressure forces direct outward from the core, and also toward the pole and equator. The magnetic field responsible for inflating the bubble is generated by the rotation of the core. Thus we are seeing the spin energy of the core being converted into linear kinetic energy of the envelope (and the core will spin down, as a result).

We have run several simulations with different relative values of $v_{\rm rot}$, $v_{\rm A}$, and $v_{\rm esc}$. We find that the envelope will be fully ejected from the system, as long as the dimensionless parameter $v_{\rm rot} v_{\rm A} v_{\rm esc}^{-2} \gtrsim 0.1$. For smaller values, the outburst may occur only at selected latitudes (e.g., the pole and equator), or, for very small values, there is no envelope ejection. For cases where the envelope is ejected, the expansion speed of the swept up shell is approximately twice the rotation speed, $v_{\rm rot}$. Also, various shell shapes are produced, with different relative speeds in the polar and equatorial regions.

The enhanced equatorial flow is a feature of the spinning dipole field. Different field geometries will not necessarily have an equatorial enhancement, though there will always be a polar enhancement. To demonstrate this more clearly, we ran a simulation with the same parameters as the data in figures 1 and 2, but with a split monopole field geometry (radial magnetic field, but with a direction reversal at the equator). The right panel of figure 3 shows the split monopole case after three rotations of the core. For comparison, the left panel shows the dipole case (same as the lower right panel of fig. 2).

3. Discussion

The magnetic explosion mechanism presented here, if triggered at the end of the AGB phase, may solve all of the problems discussed in section 1. Triggering requires that the field and the rotation of the core must either be sustained

throughout the lifetime of the AGB phase or be generated near the end of the AGB phase, perhaps stimulated by binary interaction. To compare our simulations to real pPNe, we can scale our parameters to real values. For example, we can assume a core mass of $0.5M_\odot$, a swept up shell mass and size of $0.062M_\odot$ and 10^4 AU (for CRL 2688, Bujarrabal et al., 2001, see also Kastner in these proceedings), and $v_{\rm esc} = 1000$ km s^{-1}. In that case, the simulation presented in figures 1 and 2 applies to a core with a radius of $0.2R_\odot$, $v_{\rm rot} = 100$ km s^{-1}, and a dipole field strength of 2×10^5 Gauss. If instead we assume $v_{\rm esc} = 3000$ km s^{-1}, the same simulation applies to a core with a radius of 10^9 cm, $v_{\rm rot} = 300$ km s^{-1}, and a dipole field strength of 10^8 Gauss.

The time taken to extract all of the rotational kinetic energy from the core (i.e., the spin-down time) is ~ 100 years, comparable to the typical pPNe lifetime. This may explain the short acceleration times apparent in pPNe outflows and the relative lack of quickly rotating white dwarfs (Koester et al., 1998).

Acknowledgments. We thank the organizers for a productive and enjoyable meeting. This research was supported by NSERC, McMaster University, and CITA through a CITA National Fellowship.

References

Alcolea, J., Bujarrabal, V., Sánchez Contreras, C., Neri, R., & Zweigle, J. 2001, A&A, 373, 932

Balick, B. 1987, AJ, 94, 671

Balick, B., & Frank, A. 2002, ARA&A, 40, 439

Balick, B., Wilson, J., & Hajian, A. R. 2001, AJ, 121, 354

Blackman, E. G., Frank, A., Markiel, J. A., Thomas, J. H., & Van Horn, H. M. 2001, Nature, 409, 485

Bujarrabal, V., Castro-Carrizo, A., Alcolea, J., & Sánchez Contreras, C. 2001, A&A, 377, 868

Chevalier, R. A., & Luo, D. 1994, ApJ, 421, 225

García-Segura, G., Langer, N., Różyczka, M., & Franco, J. 1999, ApJ, 517, 767

Knapp, G. R. 1986, ApJ, 311, 731

Koester, D., Dreizler, S., Weidemann, V., & Allard, N. F. 1998, A&A, 338, 612

Kwok, S., Purton, C. R., & Fitzgerald, P. M. 1978, ApJ, 219, L125

Matt, S. P. 2002, Ph.D. Thesis, Astronomy, University of Washington

Terzian, Y., & Hajian, A. R. 2000, in ASP Conf. Ser. 199: Asymmetrical Planetary Nebulae II: From Origins to Microstructures, 33